Supplementary Information

Yi-Zhuang You[1] and Ashvin Vishwanath[1]

[1] *Department of Physics, Harvard University, Cambridge, MA 02138, USA*

I. FERMION BILINEAR OPERATORS AND LOCAL INTERACTIONS

On a single orbital, the electron carries valley and spin degrees of freedom and can be written in the Majorana basis as

$$\chi = \begin{bmatrix} K \\ K' \end{bmatrix} \otimes \begin{bmatrix} \uparrow \\ \downarrow \end{bmatrix} \otimes \begin{bmatrix} \mathrm{Re}\, c \\ \mathrm{Im}\, c \end{bmatrix}. \tag{1}$$

The Majorana basis spans an 8-dimensional single-particle Hilbert space, in which there are altogether 28 fermion bilinear operators (as there are only 28 antisymmetric 8×8 matrices), which can be generally expressed as $\frac{1}{2}\chi^\intercal \sigma^{abc}\chi$ in terms of the Pauli operator $\sigma^{abc}\equiv\sigma^a\otimes\sigma^b\otimes\sigma^c$ (for $a,b,c=0,1,2,3$) with the constraint that $(\sigma^{abc})^\intercal = -\sigma^{abc}$. These operators can be classified according to their representations under the symmetry group $\mathrm{U}(4)=\mathrm{U}(1)_c\times\mathrm{SU}(4)$ or $\mathrm{U}(1)_c\times\mathrm{U}(1)_v\times\mathrm{SO}(4)$, as summarized in Tab. I.

TABLE I. The number indicates the dimension of the representation (not irreducible for U(1) groups). The subscript labels the representation: U(1) group representations are labeled by their quantum numbers $q=0$ or $q=2$, non-Abelian group representations are labeled by names (sc - scalar, ve - vector, ad - adjoint, pv - pseudo-vector, ps - pseudo-scalar).

$\mathrm{U}(1)_c$	$\mathrm{SU}(4)$	$\mathrm{U}(1)_v$	$\mathrm{SO}(4)$	operator		order parameter
16_0	1_{sc}	1_0	1_{sc}	n_c	σ^{002}	charge density
	15_{ad}	7_0	1_{ps}	n_v	σ^{302}	valley density
			6_{ad}	$\boldsymbol{S}_K \pm \boldsymbol{S}_{K'}$	$\sigma^{012},\sigma^{020},\sigma^{032}$ $\sigma^{312},\sigma^{320},\sigma^{332}$	spin (FM/AFM between valleys)
		8_2	4_{ve}	I^μ_x	$\sigma^{102},\sigma^{210},\sigma^{222},\sigma^{230}$	IVC×(charge, spin)
			4_{pv}	I^μ_y	$-\sigma^{200},\sigma^{112},\sigma^{120},\sigma^{132}$	
12_2	6_{ve}	4_0	4_{ve}	$\mathrm{Re}\,\Delta^\mu$	$-\sigma^{121},\sigma^{233},-\sigma^{201},-\sigma^{213}$	inter-valley SC
		2_2	1_{sc}	$\mathrm{Re}(\Delta_K+\Delta_{K'})$	$-\sigma^{021}$	intra-valley SC
			1_{ps}	$\mathrm{Im}(\Delta_K-\Delta_{K'})$	σ^{323}	
	6_{pv}	4_0	4_{pv}	$\mathrm{Im}\,\Delta^\mu$	$\sigma^{123},\sigma^{231},\sigma^{203},-\sigma^{211}$	inter-valley SC
		2_2	1_{sc}	$\mathrm{Im}(\Delta_K+\Delta_{K'})$	σ^{023}	intra-valley SC
			1_{ps}	$\mathrm{Re}(\Delta_K-\Delta_{K'})$	$-\sigma^{321}$	

One may therefore expect that the most generic $\mathrm{U}(1)_c\times\mathrm{U}(1)_v\times\mathrm{SO}(4)$ local interaction to be a linear combination of n_c^2, n_v^2, $\boldsymbol{S}_K^2+\boldsymbol{S}_{K'}^2$, $I^{\mu\dagger}I^\mu$ (with $I^\mu=I^\mu_x+\mathrm{i}I^\mu_y$), $\Delta^{\mu\dagger}\Delta^\mu$, $\Delta_K^\dagger\Delta_K+\Delta_{K'}^\dagger\Delta_{K'}$ (exhausting all Fermion bilinear channels). However, these interaction terms are not linearly independent, as can be seen from

$$\begin{aligned}
\frac{1}{4}(n_c^2+n_v^2) &= -\frac{1}{6}(\boldsymbol{S}_K^2+\boldsymbol{S}_{K'}^2) = \frac{1}{4}(\Delta_K^\dagger\Delta_K+\Delta_{K'}^\dagger\Delta_{K'}) = n_{K\uparrow}n_{K\downarrow}+n_{K'\uparrow}n_{K'\downarrow},\\
\frac{1}{4}(n_c^2-n_v^2) &= -\frac{1}{8}I^{\mu\dagger}I^\mu = \frac{1}{8}\Delta^{\mu\dagger}\Delta^\mu = (n_{K\uparrow}+n_{K\downarrow})(n_{K'\uparrow}+n_{K'\downarrow}).
\end{aligned} \tag{2}$$

There are only two linearly independent local interactions, so the most generic local interaction should be

$$H_{\mathrm{int}} = U_0(n_{K\uparrow}+n_{K\downarrow})(n_{K'\uparrow}+n_{K'\downarrow}) + U_1(n_{K\uparrow}n_{K\downarrow}+n_{K'\uparrow}n_{K'\downarrow}). \tag{3}$$

II. LANDAU-GINZBURG THEORY

In this appendix, we review the derivation of Landau-Ginzburg theory in Ref. 1 and propose a generalization beyond the mean-field framework. Our starting point is the BCS mean-field theory, described by the BdG Hamiltonian

$$\begin{aligned} H_{\mathrm{BdG}} &= \sum_{\boldsymbol{k}} \psi_{\boldsymbol{k}}^\dagger h_{\mathrm{BdG}} \psi_{\boldsymbol{k}}, \\ h_{\mathrm{BdG}} &= \begin{bmatrix} \epsilon_{\boldsymbol{k}} & \Delta_{\boldsymbol{k}}^\dagger \\ \Delta_{\boldsymbol{k}} & -\epsilon_{\boldsymbol{k}} \end{bmatrix}, \psi_{\boldsymbol{k}} = \begin{bmatrix} c_{K\boldsymbol{k}} \\ \mathrm{i}\sigma^2 c_{K'-\boldsymbol{k}}^\dagger \end{bmatrix}, \end{aligned} \tag{4}$$

where $c_{K\boldsymbol{k}} = (c_{K\boldsymbol{k}\uparrow}, c_{K\boldsymbol{k}\downarrow})^\intercal$ describes the electrons around the K valley and similarly for $c_{K'\boldsymbol{k}}$. The elements $\epsilon_{\boldsymbol{k}}$ and $\Delta_{\boldsymbol{k}}$ in h_{BdG} are themself 2×2 matrices. We take the single band model proposed in the main text: $\epsilon_{\boldsymbol{k}} = (\boldsymbol{k}^2 - \mu + \alpha(k_x^2 - 3k_x k_y^2))\sigma^0$. We consider the inter-valley pairing term $\Delta_{\boldsymbol{k}}$, which can be decomposed in O(4) components $\Delta_{\boldsymbol{k}}^\mu$, and each component is a linear combination of the leading form factors $w_{\boldsymbol{k}}$ and $w_{\boldsymbol{k}}^*$,

$$\Delta_{\boldsymbol{k}} = \Delta_{\boldsymbol{k}}^\mu s^\mu = w_{\boldsymbol{k}} u^\mu s^\mu + w_{\boldsymbol{k}}^* v^\mu s^\mu, \tag{5}$$

where $(s^0, \boldsymbol{s}) = (\sigma^0, -\mathrm{i}\boldsymbol{\sigma})$ and u^μ, v^μ form complex four-component vectors. Since $\epsilon_{\boldsymbol{k}}$ is proportional to an identity matrix in the spin space, so the pairing gap is purely determined by the singular value of $\Delta_{\boldsymbol{k}}$. As $\Delta_{\boldsymbol{k}}$ is a 2×2 matrix, it will have two singular values, denoted as $\delta_{n\boldsymbol{k}}$ $(n = 1, 2)$, corresponding to the gap for two different spin components (along certain direction determined by the singular vectors). These two singular values must be optimized independently, so the Landau-Ginzburg free energy should take the following form (to the quartic order of $\delta_{n\boldsymbol{k}}$)

$$F = \sum_{n=1,2}\sum_{\boldsymbol{k}} r\delta_{n\boldsymbol{k}}^2 + \kappa\delta_{n\boldsymbol{k}}^4 + \cdots = \sum_{\boldsymbol{k}} r\,\mathrm{Tr}\,\Delta_{\boldsymbol{k}}^\dagger\Delta_{\boldsymbol{k}} + \kappa\,\mathrm{Tr}\,\Delta_{\boldsymbol{k}}^\dagger\Delta_{\boldsymbol{k}}\Delta_{\boldsymbol{k}}^\dagger\Delta_{\boldsymbol{k}} + \cdots. \tag{6}$$

Plugging in Eq. (9), the above free energy reduces to

$$\begin{aligned} F &= \sum_{\boldsymbol{k}} r\Delta_{\boldsymbol{k}}^{\mu*}\Delta_{\boldsymbol{k}}^\mu + \kappa(2(\Delta_{\boldsymbol{k}}^{\mu*}\Delta_{\boldsymbol{k}}^\mu)^2 - |\Delta_{\boldsymbol{k}}^\mu\Delta_{\boldsymbol{k}}^\mu|^2) + \cdots \\ &= \tilde{r}(u^{\mu*}u^\mu + v^{\mu*}v^\mu) + \tilde{\kappa}(2(u^{\mu*}u^\mu + v^{\mu*}v^\mu)^2 + 4|u^{\mu*}v^\mu|^2 - 4|u^\mu v^\mu|^2 - |u^\mu u^\mu|^2 - |v^\mu v^\mu|^2) + \cdots \end{aligned} \tag{7}$$

where the effective parameters are give by $\tilde{r} = r\sum_{\boldsymbol{k}\in\mathrm{FS}} w_{\boldsymbol{k}}^* w_{\boldsymbol{k}}$ and $\tilde{\kappa} = \kappa\sum_{\boldsymbol{k}\in\mathrm{FS}}(w_{\boldsymbol{k}}^* w_{\boldsymbol{k}})^2$. No matter what is the particular choice of the pairing form factor $w_{\boldsymbol{k}}$, $\tilde{r}$ and $\tilde{\kappa}$ always keep the same sign as r and κ. The SC phase will correspond to the parameter regime of $\tilde{r} < 0$ and $\tilde{\kappa} > 0$. Within this parameter regime, we can minimize the free energy F with respect to u^μ, v^μ. Only two distinct class of solutions are found: the chiral solution and the helical solution. They are degenerated in the free energy.

It turns out the above mean-field framework can not provide a solution for nematic superconductivity. Within the mean-field approach, as can be seen from Eq. (11), the Landau-Ginzburg free energy is simply a sum of the contributions from the order parameter $\Delta_{\boldsymbol{k}}$ at each momentum $\boldsymbol{k}$ independently. There is no interaction between the order parameters at different momenta. However such interaction in general could exist, which can be model by a more general free energy of the following form

$$\begin{aligned} F &= \sum_{\boldsymbol{k}} r\Delta_{\boldsymbol{k}}^{\mu*}\Delta_{\boldsymbol{k}}^\mu + \sum_{\boldsymbol{k},\boldsymbol{k}'} \kappa_{\boldsymbol{k}\boldsymbol{k}'}(2\Delta_{\boldsymbol{k}}^{\mu*}\Delta_{\boldsymbol{k}}^\mu\Delta_{\boldsymbol{k}'}^{\nu*}\Delta_{\boldsymbol{k}'}^\nu - \Delta_{\boldsymbol{k}}^{\mu*}\Delta_{\boldsymbol{k}}^{\mu*}\Delta_{\boldsymbol{k}'}^\nu\Delta_{\boldsymbol{k}'}^\nu) + \cdots \\ &= \tilde{r}(u^{\mu*}u^\mu + v^{\mu*}v^\mu) + 2\tilde{\kappa}_1(u^{\mu*}u^\mu + v^{\mu*}v^\mu)^2 + 4\tilde{\kappa}_2|u^{\mu*}v^\mu|^2 - 2(\tilde{\kappa}_1 + \tilde{\kappa}_2)|u^\mu v^\mu|^2 - \tilde{\kappa}_1(|u^\mu u^\mu|^2 + |v^\mu v^\mu|^2) + \cdots. \end{aligned} \tag{8}$$

The momentum dependent coupling $\kappa_{\boldsymbol{k}\boldsymbol{k}'}$ describes the residual interaction between Cooper pairs, which would correspond to some eight-fermion interactions. Such interactions were not explicitly given in the model Hamiltonian, but they could definitely be generated under renormalization. In the case of $\kappa_{\boldsymbol{k}\boldsymbol{k}'} = \kappa\delta_{\boldsymbol{k}\boldsymbol{k}'}$, the free energy model Eq. (12) reduces to Eq. (11). The generalized model in Eq. (12) has more parameters to tune: $\tilde{\kappa}_1 = \sum_{\boldsymbol{k},\boldsymbol{k}'\in\mathrm{FS}} \kappa_{\boldsymbol{k}\boldsymbol{k}'} w_{\boldsymbol{k}}^* w_{\boldsymbol{k}} w_{\boldsymbol{k}'}^* w_{\boldsymbol{k}'}$ and $\tilde{\kappa}_2 = \sum_{\boldsymbol{k},\boldsymbol{k}'\in\mathrm{FS}} \kappa_{\boldsymbol{k}\boldsymbol{k}'}(w_{\boldsymbol{k}}^* w_{\boldsymbol{k}'})^2$. It is found that as long as $\tilde{\kappa}_2 < 0$, the nematic solution always minimizes the free energy. The solution is given in the main text.

To understand the possible scenario in which the nematic superconductivity might be favored, let us consider the following model of $\kappa_{\boldsymbol{k}\boldsymbol{k}'}$

$$\kappa_{\boldsymbol{k}\boldsymbol{k}'} = \frac{\kappa\Gamma^2}{(|\boldsymbol{k} - \boldsymbol{k}'| - Q)^2 + \Gamma^2}. \tag{9}$$

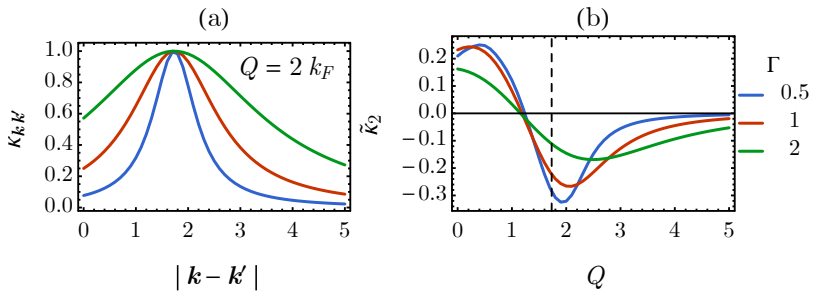

FIG. 1. (a) Dependence of $\kappa_{\boldsymbol{k}\boldsymbol{k}'}$ on $|\boldsymbol{k}-\boldsymbol{k}'|$ for different Γ. (b) $\tilde{\kappa}_2$ v.s. Q for different Γ.

We assume that the interaction between Cooper pairs could depend on the difference between their relative (not center-of-mass) momenta $\boldsymbol{k}-\boldsymbol{k}'$. Suppose $\kappa_{\boldsymbol{k}\boldsymbol{k}'}$ has a non-trivial dependence on $\boldsymbol{k}-\boldsymbol{k}'$ which peaks around $|\boldsymbol{k}-\boldsymbol{k}'| \simeq Q$ with the width of the peak controlled by a parameter Γ, see Fig. 3(a) for examples. An argument for such non-trivial momentum dependence is to note that when $Q \sim 2k_F$ (where $k_F \sim \sqrt{3\mu}$ is a crude notion of Fermi momentum even if the Fermi surface is not of circular shape), the Cooper pairs $\Delta^{\mu}_{k_F}$ and $\Delta^{\mu}_{-k_F}$ coincide and repel each other strongly, leading to a resonance of the repulsive interaction around $Q \sim 2k_F$. To ensure the stability of the Landau-Ginzburg theory, the quartic term would better be positive, i.e. $\kappa_{\boldsymbol{k}\boldsymbol{k}'} > 0$. In terms of the model in Eq. (13), it corresponds to setting $\kappa > 0$. The precise form of $\kappa_{\boldsymbol{k}\boldsymbol{k}'}$ relies on many details, but the simple toy model in Eq. (13) already serves the purpose to show an important fact: it is possible to gain attractive interaction $\tilde{\kappa}_2 < 0$ even if $\kappa_{\boldsymbol{k}\boldsymbol{k}'} > 0$ is always repulsive, as long as $\kappa_{\boldsymbol{k}\boldsymbol{k}'}$ has sufficiently non-trivial momentum dependence. Recall that $\tilde{\kappa}_2 < 0$ is all we need to stabilize the nematic superconductivity in the free energy analysis. To show this, we take the generic form factor $w_{\boldsymbol{k}} = w_d k_+^2 + w_p k_-$ for a mixed $d+\mathrm{i}d$ and $p-\mathrm{i}p$ pairing, and calculate the coefficient $\tilde{\kappa}_2$ for different values of Q and Γ. The result is shown in Fig. 3(b). It demonstrates that around $Q \sim 2k_F$, $\tilde{\kappa}_2$ indeed becomes negative. However this behavior heavily relies on the form of $\kappa_{\boldsymbol{k}\boldsymbol{k}'}$: if $\kappa_{\boldsymbol{k}\boldsymbol{k}'}$ does not peak around a sufficiently large momentum Q (for example $Q \to 0$), then $\tilde{\kappa}_2$ will be positive and not favoring the nematic superconductivity.

III. SELF-CONSISTENT MEAN-FIELD THEORY

We provide here the details about the self-consistent mean-field theory to capture the competition between the IVCW and the TSC orders. Our starting point is the mean-field Hamiltonian H_{MF} in the main text, which can be written in a more convenient form by introducing the fermion $\psi_{\boldsymbol{k}} = (c_{K\boldsymbol{k}\uparrow}, c^{\dagger}_{K'-\boldsymbol{k}\downarrow}, c_{K'\boldsymbol{k}-\boldsymbol{Q}\uparrow}, c^{\dagger}_{K-\boldsymbol{k}+\boldsymbol{Q}\downarrow})^{\intercal}$, such that

$$\begin{aligned} H_{\mathrm{MF}} &= \sum_{\boldsymbol{k}} \psi^{\dagger}_{\boldsymbol{k}} h_{\boldsymbol{k}} \psi_{\boldsymbol{k}} + H_{\mathrm{bg}}, \\ H_{\mathrm{bg}} &= +g_I I^{0*}_{\boldsymbol{Q}} I^{0}_{\boldsymbol{Q}} - g_{\Delta} \sum_{\boldsymbol{k}} \Delta^{0*}_{-\boldsymbol{k}+\boldsymbol{Q}} \Delta^{0}_{\boldsymbol{k}}, \\ h_{\boldsymbol{k}} &= \begin{bmatrix} \epsilon_{\boldsymbol{k}} & -g_{\Delta}\Delta^{0}_{\boldsymbol{k}} & g_I I^{0*}_{\boldsymbol{Q}} & 0 \\ -g_{\Delta}\Delta^{0*}_{\boldsymbol{k}} & -\epsilon_{\boldsymbol{k}} & 0 & -g_I I^{0*}_{\boldsymbol{Q}} \\ g_I I^{0}_{\boldsymbol{Q}} & 0 & \epsilon_{-\boldsymbol{k}+\boldsymbol{Q}} & -g_{\Delta}\Delta^{0}_{-\boldsymbol{k}+\boldsymbol{Q}} \\ 0 & -g_I I^{0}_{\boldsymbol{Q}} & -g_{\Delta}\Delta^{0*}_{-\boldsymbol{k}+\boldsymbol{Q}} & -\epsilon_{-\boldsymbol{k}+\boldsymbol{Q}} \end{bmatrix}. \end{aligned} \tag{10}$$

We will take single-orbital model $\epsilon = \boldsymbol{k}^2 - \mu + \alpha\,\mathrm{Re}\,k_+^3$ with $\alpha = 1/3$. $I^0_{\boldsymbol{Q}}$ and $\Delta^0_{\boldsymbol{k}}$ are order parameters subject to optimization, where $I^0_{\boldsymbol{Q}}$ is treated as a constant independent of the momentum $\boldsymbol{k}$ while $\Delta^0_{\boldsymbol{k}}$ is a function of $\boldsymbol{k}$. To proceed, we focus on a patch of the momentum space that is large enough to cover the Fermi pockets, and we discretize the momentum patch to a triangular grid (to preserve the C_3 rotation symmetry) of $3L^2$ momentum points with $L = 12$, see Fig. 1(b) for the illustration of momentum grid. We diagonalize the mean-field Hamiltonian at each momentum $\boldsymbol{k}$ to obtain the eigen energy $E_{n\boldsymbol{k}}$, s.t. $h_{\boldsymbol{k}}|n\rangle = E_{n\boldsymbol{k}}|n\rangle$. The free energy of the fermion can be evaluated from $E_{n\boldsymbol{k}}$ as

$$F_{\mathrm{MF}} = -\beta^{-1} \sum_{n\boldsymbol{k}} \ln(1 + e^{-\beta E_{n\boldsymbol{k}}}) + H_{\mathrm{bg}}. \tag{11}$$

The free energy F_{MF} is a function of the order parameters $I^0_{\boldsymbol{Q}}, \Delta^0_{\boldsymbol{k}}$. Given the temperature T and the chemical potential μ, we can find the optimal configuration of the order parameters that minimize F_{MF}. For example, Fig. 1 shows one typical result of the mean-field iteration in the TSC phase. The $d+\mathrm{i}d$ and $p-\mathrm{i}p$ mixed paring form factor is clearly seen from Fig. 1(b), consistent with the result in Fig. 5(b) obtained by a different method (by solving the gap equation). Repeating this calculation, we can find the mean-field solution numerically throughout the phase diagram.

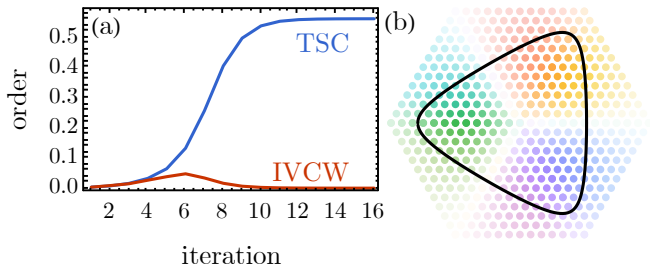

FIG. 2. (a) Self-consistent mean-field iteration showing the development and the convergence of the IVCW and the TSC order parameters. (b) The obtained gap function $\Delta^0_{\boldsymbol{k}}$ in the momentum space (around the K pocket). Each dot represent a momentum point $\boldsymbol{k}$ on the momentum grid. The color indicates the phase of $\Delta^0_{\boldsymbol{k}}$, following the color scheme of Fig. **??**. The black curve marks out the shape of the K pocket.

It is found that the IVCW order $I^0_{\boldsymbol{Q}}$ and the TSC order $\Delta^0_{\boldsymbol{k}}$ never coexist in the phase diagram. In fact, they are not expected to coexist, because they are commuting order parameters that always compete for Fermi surface density of state. This mechanism can be understood from a simplified toy model. In the case of perfect nesting, we have $\Delta^0_{\boldsymbol{k}} = -\Delta^0_{-\boldsymbol{k}+\boldsymbol{Q}}$ and $\epsilon_{\boldsymbol{k}} = -\epsilon_{-\boldsymbol{k}+\boldsymbol{Q}}$. Let us ignore the momentum dependence along the Fermi surface and simply set $\epsilon_{\boldsymbol{k}} = k_\perp$ ($k_\perp$ is the momentum perpendicular to the Fermi surface), $-g_\Delta \Delta^0_{\boldsymbol{k}} = m_\Delta$, $g_I I^0_{\boldsymbol{Q}} = m_I$, then the mean-field single-particle Hamiltonian $h_{\boldsymbol{k}}$ in Eq. (4) takes the form of

$$h = \begin{bmatrix} k_\perp & m_\Delta & m_I & 0 \\ m_\Delta & -k_\perp & 0 & -m_I \\ m_I & 0 & -k_\perp & -m_\Delta \\ 0 & -m_I & -m_\Delta & k_\perp \end{bmatrix} = k_\perp \sigma^{33} + m_I \sigma^{13} + m_\Delta \sigma^{31}. \tag{12}$$

The notation $\sigma^{ab} = \sigma^a \otimes \sigma^b$ stands for the tensor product of the Pauli matrices. m_I and m_Δ are promotional to the IVCW and the TSC gaps respectively. By saying that the two orders commute, we mean their corresponding vertex matrices σ^{13} and σ^{31} commute. As a result of the commutativity between IVCW and TSC orders, the eigenenergies of h are $\pm\sqrt{k_\perp^2 + (m_I \pm m_\Delta)^2}$, which give rise to two gaps $|m_I \pm m_\Delta|$ for the Fermi surfaces in general. However, it is energetically favorable to gap out all Fermi surfaces with the same gap size. This can be seen by evaluating the free energy at zero temperature,

$$\begin{aligned} F(m_I, m_\Delta) &\propto -\int_{-\Lambda}^{\Lambda} \mathrm{d}k_\perp \left(\sqrt{k_\perp^2 + (m_I + m_\Delta)^2} + \sqrt{k_\perp^2 + (m_I - m_\Delta)^2} \right) \\ &\simeq -\frac{1}{4}(m_I + m_\Delta)^2 \ln \frac{\Lambda^2}{(m_I + m_\Delta)^2} - \frac{1}{4}(m_I - m_\Delta)^2 \ln \frac{\Lambda^2}{(m_I - m_\Delta)^2}. \end{aligned} \tag{13}$$

With a choice of the momentum cutoff at $\Lambda = 1$, the free energy profile is shown in Fig. 2. One can see that the gaps (order parameters) m_I and m_Δ repel each other and the free energy is minimized only if one of them vanishes, i.e. $m_I = 0$ or $m_\Delta = 0$. Therefore the two orders are not expected to coexist.

In the self-consistent mean-field iteration of the full model in Eq. (4), we also explicitly tested the possibility of coexisting IVCW and TSC orders. We start with the initial condition that both order parameter are non-zero and providing roughly the same size of the gap. We found that under the self-consistent iteration (equivalent to the gradient decent to minimize the free energy), the oder parameter always flow to either the IVCW or the TSC fixed point (with one kind of order only), see Fig. 1(a) for example. We performed this test for several different choices of the model parameters near the IVCW-TSC transition. We did not observe a mean-field saddle point with coexisting

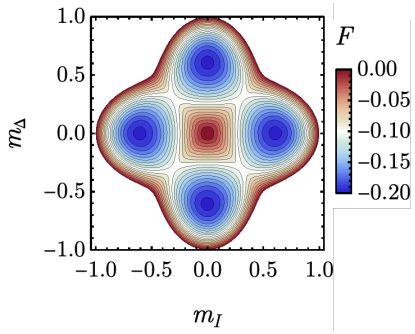

FIG. 3. Contour plot of free energy F in Eq. (7) as a function of the gaps m_I and m_Δ. The IVCW and the TSC gaps repel each other, so they can not coexist.

orders.

[1] C. Xu and L. Balents, Phys. Rev. Lett. **121**, 087001 (2018), URL https://link.aps.org/doi/10.1103/PhysRevLett.121.087001.